

## Calculation of spin- and angle-resolved photoemission spectra from Pd(100) coated with a monolayer of a magnetic 3d metal: Fe, Co, and Ni

U. König

*Institut für Technische Elektrochemie, Technische Universität Wien, A-1060 Wien, Austria*

S. Blügel

*Institut für Festkörperforschung der Kernforschungsanlage Jülich, Postfach 1913, D-5170 Jülich, Federal Republic of Germany*

J. Redinger and P. Weinberger

*Institut für Technische Elektrochemie, Technische Universität Wien, A-1060 Wien, Austria*

(Received 7 June 1990)

Using full-potential linear augmented-plane-wave film potentials, calculations of spin- and angle-resolved photoemission spectra are reported for the Pd(100) system covered with a monolayer of ferromagnetic Fe, Co, and Ni. A comparison of spin-resolved layerlike contributions to the photocurrent is given with respect to the clean Pd(100) surface. Also discussed is the occurrence of spin-resolved surface states.

### I. INTRODUCTION

3d monolayers as overlayers on metal substrates are very interesting realizations of two-dimensional magnetism. In order to investigate the Pd(100) surface coated with a monolayer of a magnetic 3d metal, we calculate spin- and angle-resolved photoemission. Blügel and co-workers<sup>1-6</sup> showed that, as far as the overlayer properties are concerned, the 3d metals V, Cr, Mn, Fe, Co, and Ni can be classified into two groups: (i) for Fe, Co, and Ni monolayers on Pd(100) a stable  $p(1 \times 1)$  ferromagnetic structure is predicted whereas (ii) for V, Cr, and Mn a stable  $c(2 \times 2)$  antiferromagnetic structure should be observed. In this paper we will deal with the ferromagnetic overlayers only, while the antiferromagnetic cases will be discussed separately.

The Pd host is expected to act differently than other noble metals. Due to the high local density of states (LDOS) at the Fermi level, hybridization between the 3d overlayer and the 4d impurity bands is expected to be strong,<sup>1-7</sup> contrary, for example, to Ag where the large gap reduces the 3d-4d hybridization.<sup>2</sup> Also it should be easy to polarize<sup>5-7</sup> the Pd matrix, since Pd is a nearly ferromagnetic metal with a large Stoner enhancement factor of about 10. For example, Mn, Fe, and Co impurities show giant moments of 10–12 $\mu_B$  when they are dissolved in Pd.

On the surface two major effects influence the wave functions: (1) the electron wave function overlaps with a reduced number of nearest neighbors and decays exponentially into the vacuum. This reduces the bandwidth and influences of course the LDOS. Since there are fewer nearest neighbors the hybridization compared to 3d impurities dissolved in Pd should be lower; (2) the surface atom is exposed to a strong noncubic "surface

field" which removes degeneracies in the  $d$  states and leads to a considerable shift in the local energy levels. Blügel<sup>1</sup> found in LDOS of the overlayers a spin splitting being larger but otherwise similar to the elemental fer-

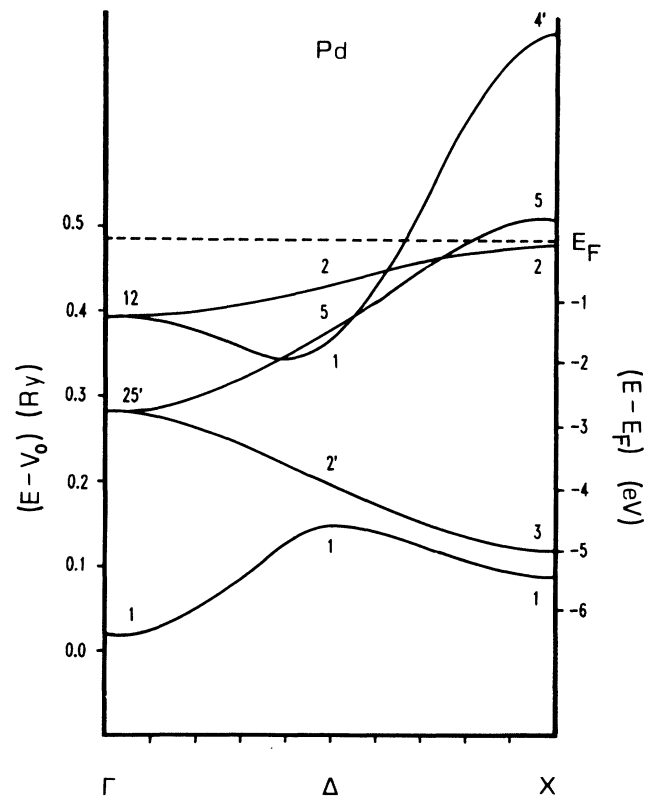


FIG. 1. Nonrelativistic LAPW bulk band structure for Pd along  $\Gamma$ - $\Delta$ - $X$  below the Fermi energy.

romagnets. Due to hybridization, however, the LDOS is of different shape than comparable bulk quantities. The hybridization is expected to be more important for the more or less filled states.

In the following we will present the spin resolved spectra for a Fe, Co, and Ni overlayer on Pd(100). The calculations are based on the (nonrelativistic) theory of angle-resolved photoemission as described by Hopkinson, Pendry, and Titterton<sup>8</sup> in which the time-reversed low-

energy electron-diffraction (LEED) formalism<sup>9,10</sup> is applied consistently, and where the bulk and the surface electronic structure are treated on equal footing. Our calculations are based on a muffin-tin-type form of the potential obtained by a scalar-relativistic full-potential augmented-plane-wave (FLAPW) thin-film calculation: in the vacuum region the  $z$ -dependent part of the FLAPW potential replaces the usual step function,<sup>10,11</sup> whereas in the crystal its layer-dependent spherical sym-

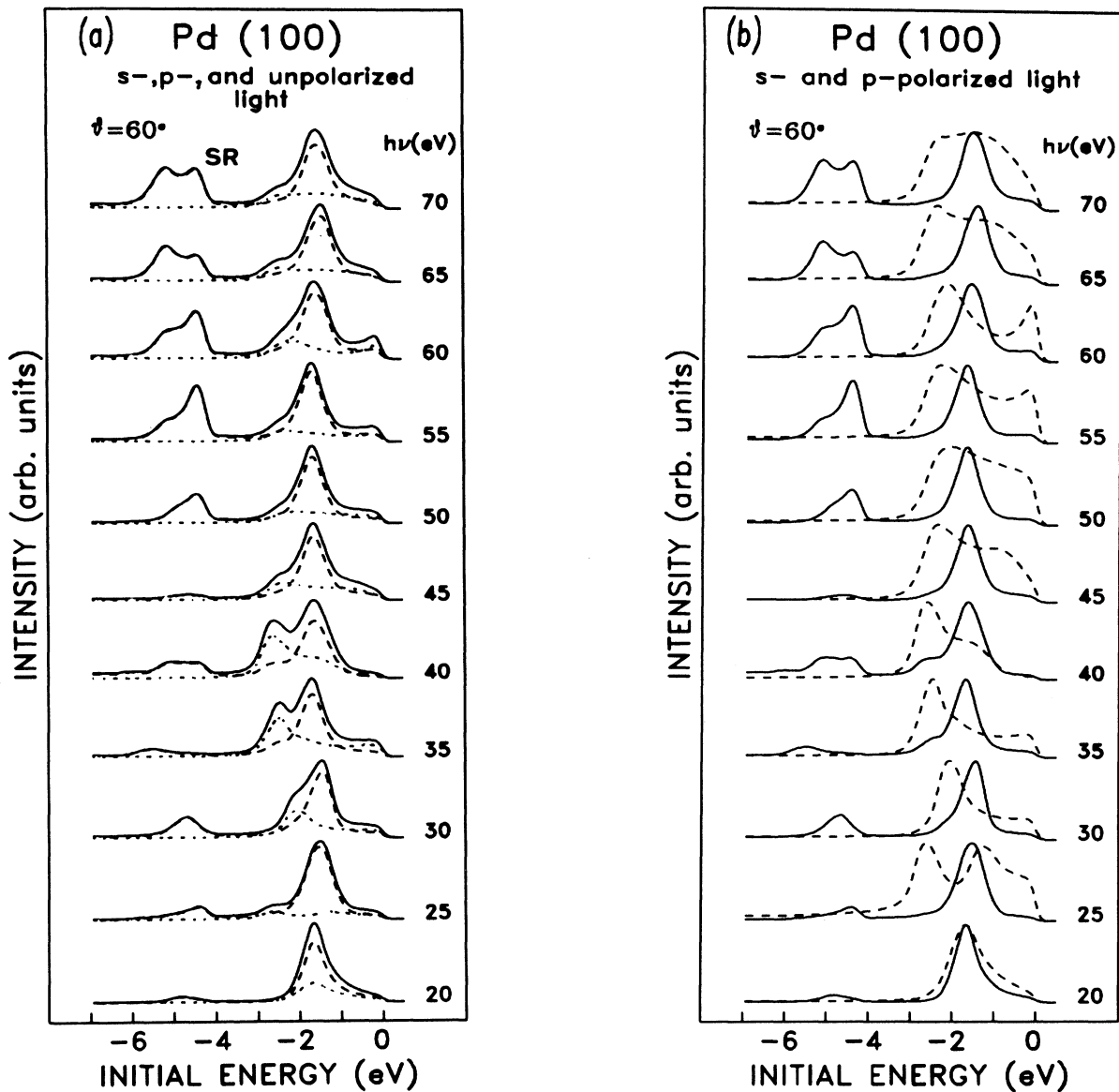


FIG. 2. Normal-emission spectra for clean Pd(100) for different energies and for an angle of incidence of  $\theta = 60^\circ$ . (a) Unpolarized light (solid line),  $s$ - (dotted line) and  $p$ -polarized light (dashed line). (b)  $s$ - (dashed line) and  $p$ -polarized (solid line) light individually normalized.

metric parts are used. Thus our calculation should provide a very realistic description of the surface properties.

## II. COMPUTATIONAL DETAILS

The FLAPW potential for Pd was calculated for a nine-layer slab. We used the FLAPW potentials from the two outermost layers to represent the surface and the subsurface layer, and the central layer potential to represent the bulk. For the overlayer systems a slab of seven layers of Pd coated with one  $3d$  layer on both sides was used. In the photocurrent calculation the highest  $l$  value for the spherical wave expansion was 4 and the number of layers was restricted to 128 for initial energies and 16 for final energies. For the  $p(1 \times 1)$  overlayer systems as well as for pure Pd 21 beams turned out to be sufficient for the convergence of the photocurrent. In or-

der to model the lifetime of the initial (hole) states an imaginary part of  $-0.14$  eV was chosen. For the final states we found that a linear dependence of the imaginary part with respect to photon energy gave the best results,<sup>12</sup> namely a variation from  $-1$  eV at 20 eV to  $-4$  eV at 70 eV photon energy.

The theoretical spectra were finally convoluted with a Gaussian spectrometer function of 0.2 eV full width at half maximum and individually normalized to the highest peak. In the following all binding energies are given with respect to the Fermi level.

## III. BAND STRUCTURE OF PURE Pd

For matters of convenience and comparison we calculated a nonrelativistic LAPW bulk band structure of pure Pd (Fig. 1) along  $\Gamma$ - $\Delta$ - $X$  using the central layer of the FLAPW slab calculation. Since in Pd, as a  $4d$  element, relativistic effects can very well matter we compared the nonrelativistic LAPW bands with the corresponding scalar-relativistic LAPW bands and found that the latter are shifted by about 0.05 Ry to lower energies. Since the Fermi energy provided by the FLAPW calculation corresponds to a scalar-relativistic calculation, we adjusted the Fermi energy for our spectra such that also in the nonrelativistic calculation the Fermi level cuts between the  $X_5$  and the  $X_2$  point. As compared to a nonrelativistic APW band-structure calculation by Smith,<sup>13</sup> which was fitted to the parameters of a combined interpolation scheme, very good agreement concerning dispersion and energy levels of the high-symmetry points is found. Christensen<sup>14</sup> published a RAPW band structure and compared it to APW results by Müller *et al.*<sup>15</sup> In general our  $s$ - and  $d$ -band width and the  $s$  and  $d$  separation lie between the relativistic and nonrelativistic APW results. Except for the  $s$ -band width they are always closer to the relativistic values. It is worthwhile to mention that very good agreement between the Bloch eigenstates obtained from the photocurrent calculation and the nonrelativistic LAPW band structure was found.

## IV. PHOTOCURRENT CALCULATIONS

The photoemission spectra are calculated for normal emission and an angle of  $\theta = 60^\circ$  with respect to the surface normal for the incident light. Normal emission requires totally symmetric final-state bands, i.e.,  $\Delta_1$  symmetry, and only initial states with  $\Delta_1$  and  $\Delta_5$  symmetry can be investigated. The use of  $s$ - and  $p$ -polarized light can further restrict the selection rules.  $s$ -polarized light has only a component of the electromagnetic field vector parallel to the surface, hence only  $\Delta_5$  initial states are probed. In the case of  $p$  polarization there is a component parallel and orthogonal to the surface and  $\Delta_1$  as well as  $\Delta_5$  initial states can be seen, favoring the  $\Delta_1$  states. Full  $p$  polarization, i.e., only a component orthogonal to the surface, cannot be achieved.

Throughout this paper the spectra for unpolarized light are presented as the sum of  $s$ - and  $p$ -polarized con-

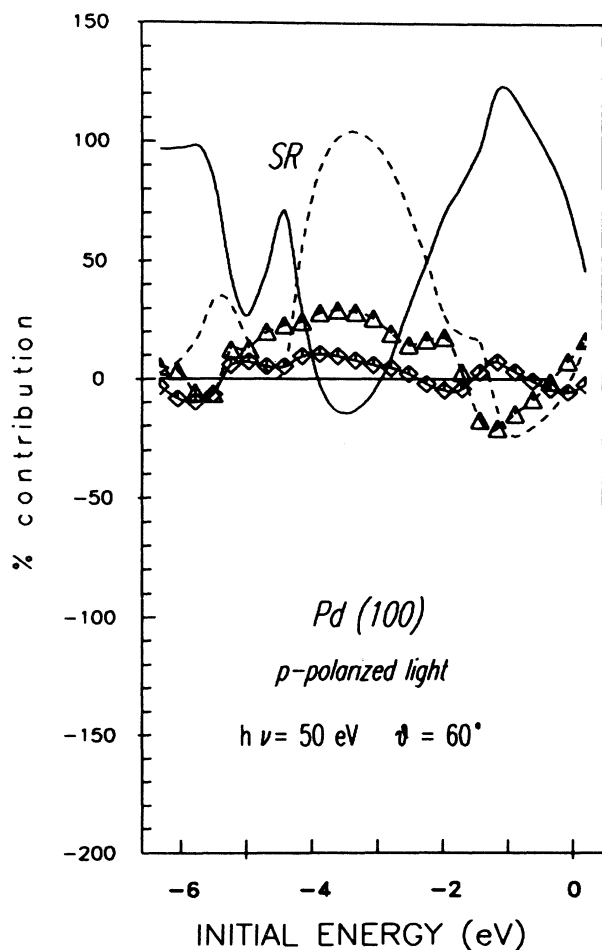


FIG. 3. Layer-by-layer distribution of the photocurrent for Pd(100) for  $p$ -polarized light at 50 eV. Solid line: layer 1; dashed line: layer 2, triangles: layer 3; squares: layer 4.

tributions and the spin-integrated spectra as the sum of minority- and majority-spin contributions. In order to get more insight in the origin of the different peaks, in some cases the layer-by-layer distribution of the photocurrent is shown. The percent contributions are then calculated with respect to the photocurrent at a certain energy. It should be noted that the contribution from the surface barrier is found to be insignificant in all cases.

### V. PHOTOEMISSION SPECTRA OF Pd(100)

Figure 2(a) shows the spectra for  $s$ -,  $p$ -, and unpolarized light, whereas in Fig. 2(b) we show both contributions in-

dividually normalized. Clearly the excitations of the  $p$ -polarized contributions dominate the spectra.

For  $s$ -polarized light there are basically three features to distinguish. The lowest peak disperses between  $-2.6$  and  $-2.0$  eV. Comparing its binding energy with a calculation using just the central layer of the FLAPW potentials exhibits no shift, thus indicating a bulklike feature. This peak originates from excitations of the  $\Delta_5$  band around  $\Gamma$  with  $|\mathbf{k}|$  extending to about the first third of the Brillouin zone. The second peak, which is visible for 20 and 25 eV photon energy at  $-1.7$  and  $-1.25$  eV binding energy, respectively, is due to a second excitation from the  $\Delta_5$  band with  $|\mathbf{k}|$  corresponding to about the

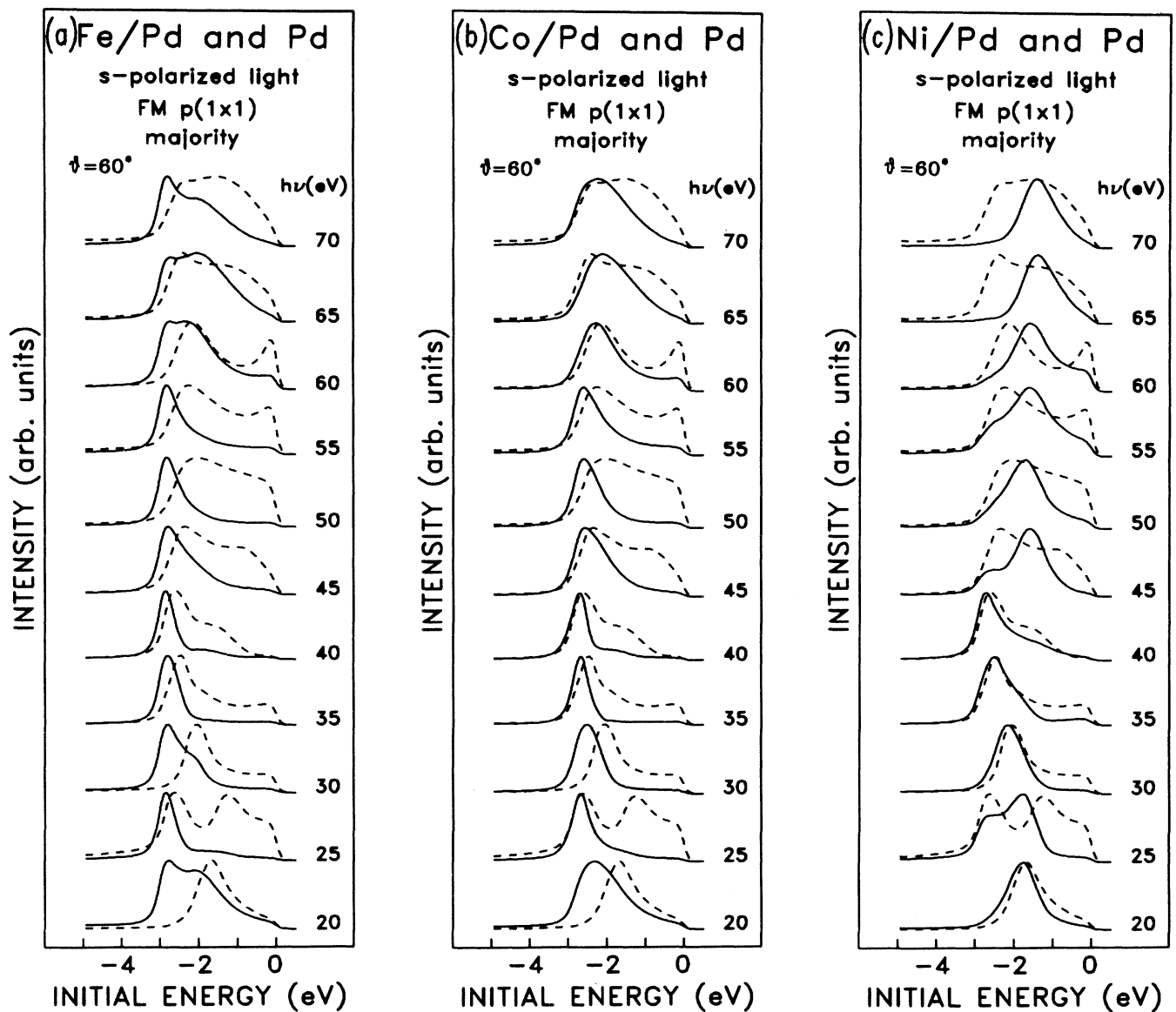


FIG. 4.  $s$ -polarized majority-spin spectra (solid lines) for (a) an Fe overlayer, (b) a Co overlayer, and (c) a Ni overlayer on Pd(100) in comparison to clean Pd(100) (dashed line).

middle of the  $\Gamma$ - $\Delta$ - $X$  line. Again the comparison with the "central-layer-only" calculation indicates a bulklike feature. However, the situation changes for higher photon energies, where a broad, strongly dispersing feature arises, which is much weaker in the "central-layer-only" calculation. Although the  $\Delta_5$  band extends up to the Fermi level and could therefore support bulklike excitations, this feature more likely is a surface resonance situated slightly above the  $\Delta_5$  band near  $\Gamma$ . Further insight in the origin of this peak is provided by the layer-by-layer distribution of the photocurrent. For 20 and 25 eV photon energy the contribution to the total current for this particular peak originates uniformly from the first four layers. However, for higher photon energies, e.g., 50 eV as shown in Fig. 3, the contribution from the first layer clearly dominates, the second layer contribution is even negative, and the third and fourth layer contributions are almost zero. The last peak is found just below the Fermi energy and it is best resolved for high photon energies.

Since it is found so close to the Fermi level it is difficult to distinguish between a dispersionless surface state, varying only in intensity, and a bulklike feature originating from the  $\Delta_5$  band with  $|\mathbf{k}|$  close to  $X_5$ . The layer-by-layer distribution indicates rather a bulklike feature. Also a comparison with other (100) surfaces gives no indication of a surface state.

In the case of  $p$ -polarized light there are four peaks visible. Comparison to the "central-layer-only" calculation shows a shift only for the surface resonance feature, labeled by SR. This feature is shifted by about 0.3 eV to higher energies and also is much better resolved in the second case. For certain photon energies its intensity is even larger than that of the lowest peak. The surface resonance is found at a binding energy of about -4.5 eV. For high photon energies the layer-by-layer distribution again shows a pronounced maximum of the first layer. This suggests an interpretation as a surface resonance split off from the lowest  $\Delta_1$  band.

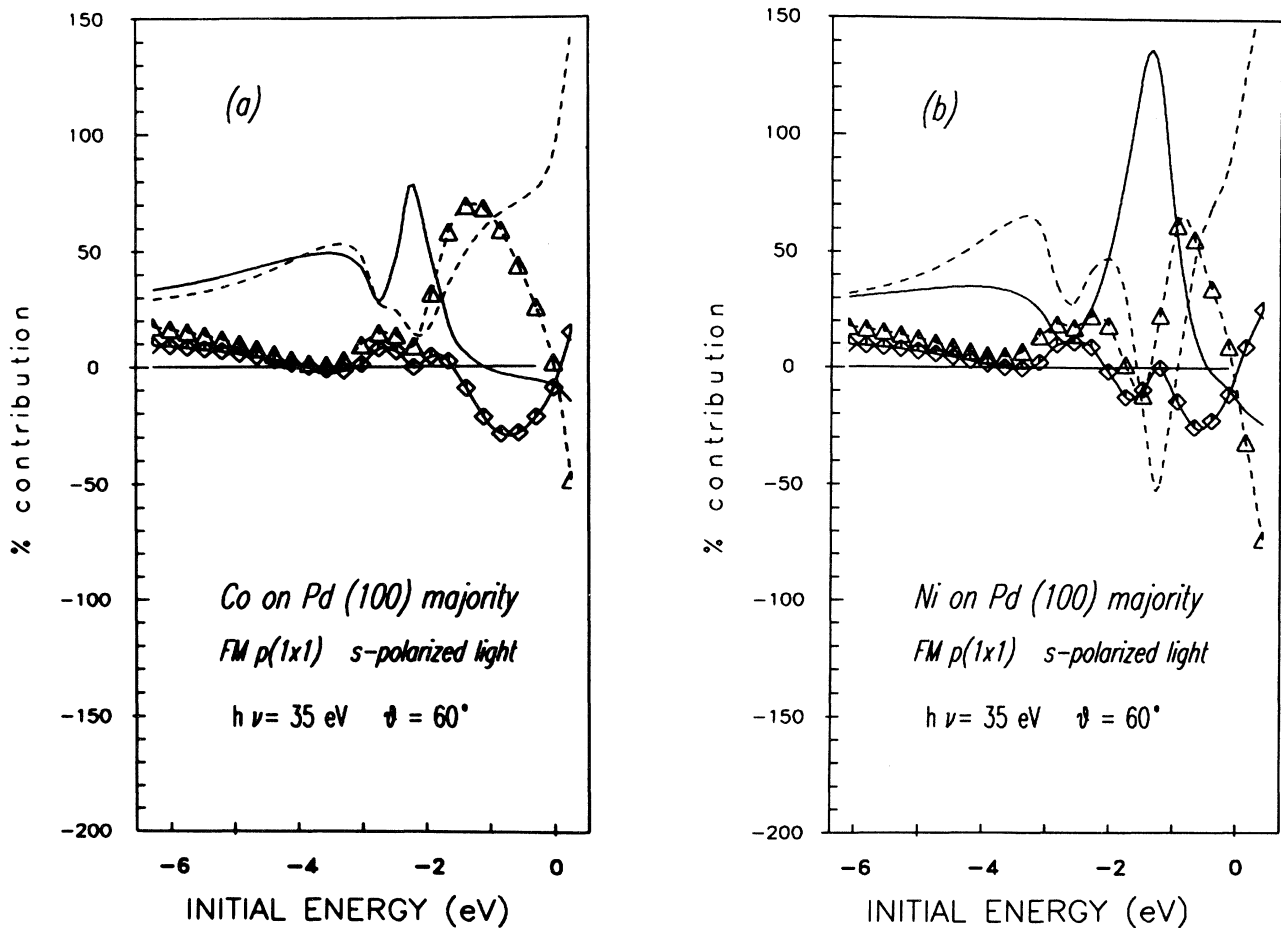


FIG. 5. Layer-by-layer distribution of the photocurrent for  $s$ -polarized light and majority spin. Solid line, layer 1 ( $3d$  metal); dashed line, layer 2 (first Pd layer); triangles, layer 3; diamonds, layer 4. (a) Co for 35 eV, (b) Ni for 35 eV, (c) Ni for 45 eV.

All other features in Figs. 2(a) and 2(b) refer to pure bulk states. The lowest peak dispersing between  $-4.7$  and  $-5.5$  eV originates from the lowest  $\Delta_1$  band with a possible range of  $|\mathbf{k}|$  extending from the middle of the  $\Gamma$ - $\Delta$ - $X$  line to  $X$ . The dominant peak of the whole spectrum is found at  $-1.4$  to  $-1.7$  eV binding energy. It originates in the  $\Delta_1$  band rather around  $\Gamma$  with  $|\mathbf{k}|$  extending possibly to the middle of the  $\Gamma$ - $\Delta$ - $X$  line. The shoulder to the left of this peak at about  $-2.6$  eV, which is only visible for the 35 and 40 eV photon energy cases, and is due to an excitation from the  $\Delta_5$  band around  $\Gamma$ .

#### A. Comparison with experiment

There are hardly any normal-emission experiments for the pure Pd(100) system. Most investigations deal with overlayer systems. For example, Smith *et al.*<sup>16</sup> present He I and He II spectra for Pd overlayers on Ag. Since Pd and Ag show little  $d$ - $d$  hybridization, the features above about  $-4$  eV binding energy can be unambiguously attri-

buted to Pd bands. They find peaks at about  $-2.4$  and  $-1.2$  eV which compare very well with our data.

Pessa and Vulli<sup>17</sup> present a spectrum of clean Pd(100) together with an investigation of Ag overlayers on Pd(100). For unpolarized light with an energy of 21.2 eV and for an incidence angle of  $15^\circ$  their normal-emission spectra show a main peak at  $-1.8$  eV and an additional small feature at  $-0.8$  eV.

O'Neill and Joyce<sup>18</sup> find in a similar investigation a Pd related peak at  $-1.8$  eV. Stulen *et al.*<sup>19</sup> studied H desorption on Pd(100). Their clean Pd spectrum, however, shows just one big hump extending from  $-2$  to  $-5$  eV. For normal emission with unpolarized light incident at an angle of  $20^\circ$  Lloyd, Quinn, and Richardson<sup>20</sup> find a peak at  $-1.8$  eV for a polycrystalline probe.

#### VI. Fe, Co, Ni—FERROMAGNETIC OVERLAYERS ON Pd(100)

In this section the majority- and minority-spin spectra are discussed separately. In the following occasionally

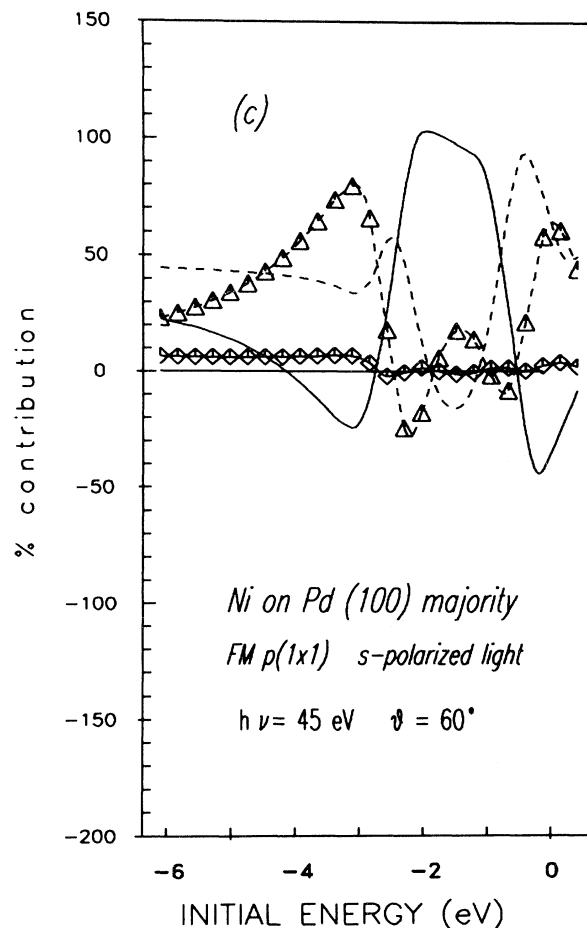


FIG. 5. (Continued).

peaks will be referred to loosely as Pd peaks although of course they are more or less hybridized to states related to the overlayers. Also the assignment of peaks refers to the traditionally used three-dimensional point-group symmetry rather than to the more appropriate two-dimensional point-group symmetry.

### A. Majority-spin direction

The majority-spin spectra for Fe and Co are very similar. For both systems we found basically the same

features and only a small shift in binding energies.

In the case of *s* polarization (Fig. 4) the lowest Pd peak, due to an excitation around  $\Gamma$ , is shifted by about 0.3–0.6 eV in the case of 30 eV photon energy compared to pure Pd. For all photon energies this peak is dominant in the majority-spin spectra and probably is due to an excitation from the Pd bulk  $\Gamma_{12}$ -like state hybridized to the Co or Fe overlayer, respectively. At 20 eV there is some deviation in the spectra for Fe: two features related to two corresponding excitations from the clean Pd(100) system become visible, whereby the higher peak is not yet resolved at 20 eV. The second peak for pure Pd and also the surface resonance discussed in Sec. V vanish for all

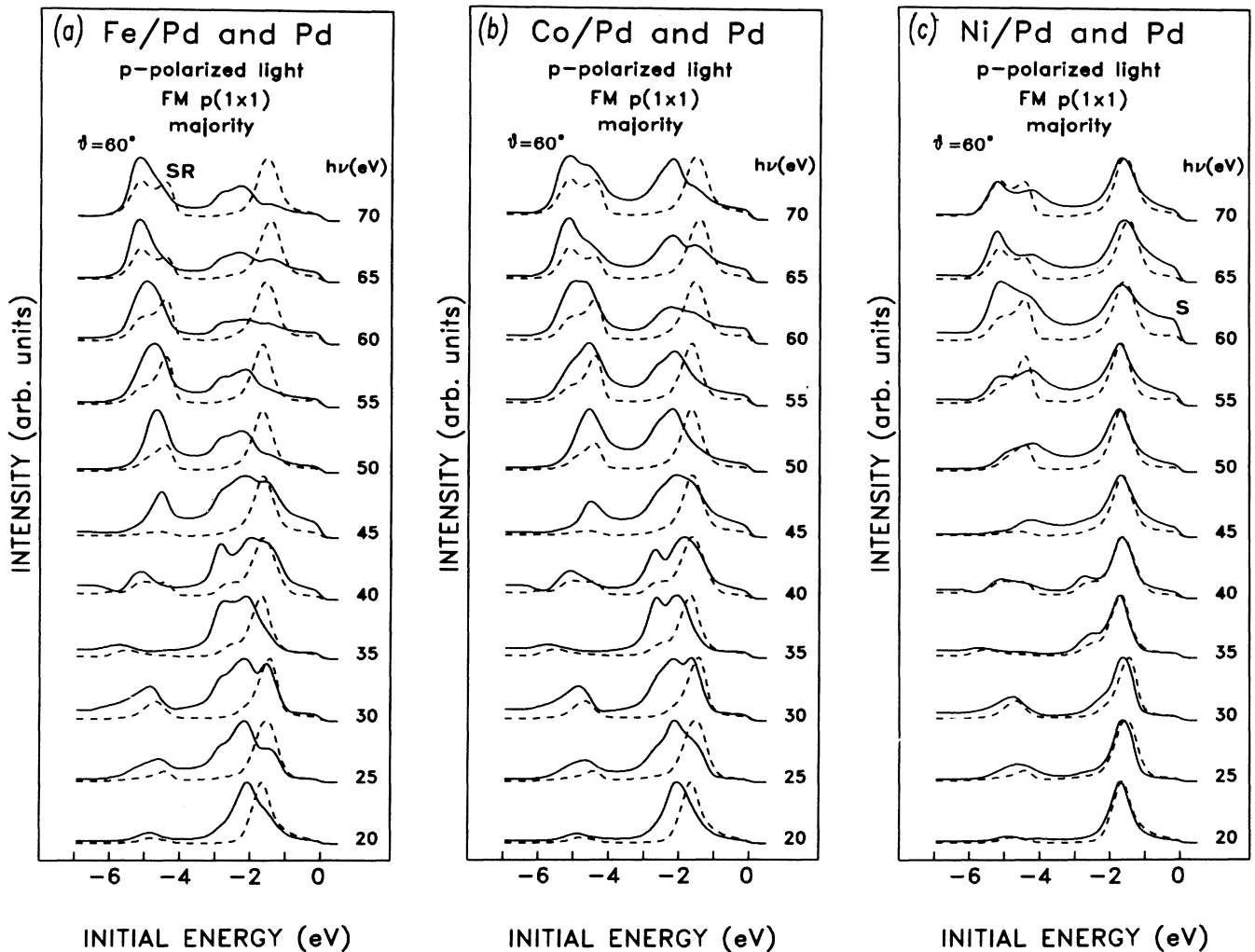


FIG. 6. *p*-polarized majority-spin spectra (solid lines) for (a) an Fe overlayer, (b) a Co overlayer, and (c) a Ni overlayer on Pd(100) in comparison to clean Pd(100) (dashed line).

other photon energies up to 55 eV. For photon energies above 55 eV the Pd related surface resonance broadens the peak in the case of Co [Fig. 4(b)] and develops a second distinct feature in the case of Fe [Fig. 4(a)]. This might be due to an enhancement of the surface resonance by the magnetic overlayer.

Ni shows different majority-spin spectra [Fig. 4(c)]. Up to 40 eV there are hardly any differences to the spectra of clean Pd(100). Only a small shift to lower energies is found (0.1 eV). Above 45 eV photon energies the Ni contribution increases, which in particular can be seen in the layer-by-layer distribution of the photocurrent in Fig. 5. At about  $-1.4$  to  $-1.7$  eV binding energy a peak develops, which eventually becomes the most prominent feature and suppresses the two Pd features. Again it is difficult to distinguish whether this peak originates from a hybridized  $\Delta_5$ -like Pd-Ni band or is related to the surface resonance of clean Pd enhanced by the Ni overlayer.

The spectra for  $p$ -polarized light are presented in Fig. 6. For Co and Fe [Figs. 6(a) and 6(b)] they show that the lowest Pd peak, due to the excitation from the lowest  $\Delta_1$  band, is least affected. As can be seen from the layer-by-layer distribution (Fig. 7) the main contributions come from the Pd layer, resembling the Pd origin of this peak. The surface resonance is broadened and shifted by about 0.2 eV to lower energies. In Fig. 7 a distinct maximum of the first layer contribution can be seen.

The peaks above  $-3$  eV binding energy are drastically changed as compared to the pure system. In between the Pd  $\Delta_5$  and  $\Delta_1$  excitations a new peak is generated, dispersing from about  $-2.0$  to  $-2.4$  eV. The Pd  $\Delta_5$  peak is more pronounced (a strong first layer contribution is found), whereas the Pd  $\Delta_1$  peak still gets most of its intensity from the lower Pd layers. The new peak must have  $\Delta_1$  symmetry as it is not observed in the  $s$ -polarized spectra. Most of its contributions are from the top lay-

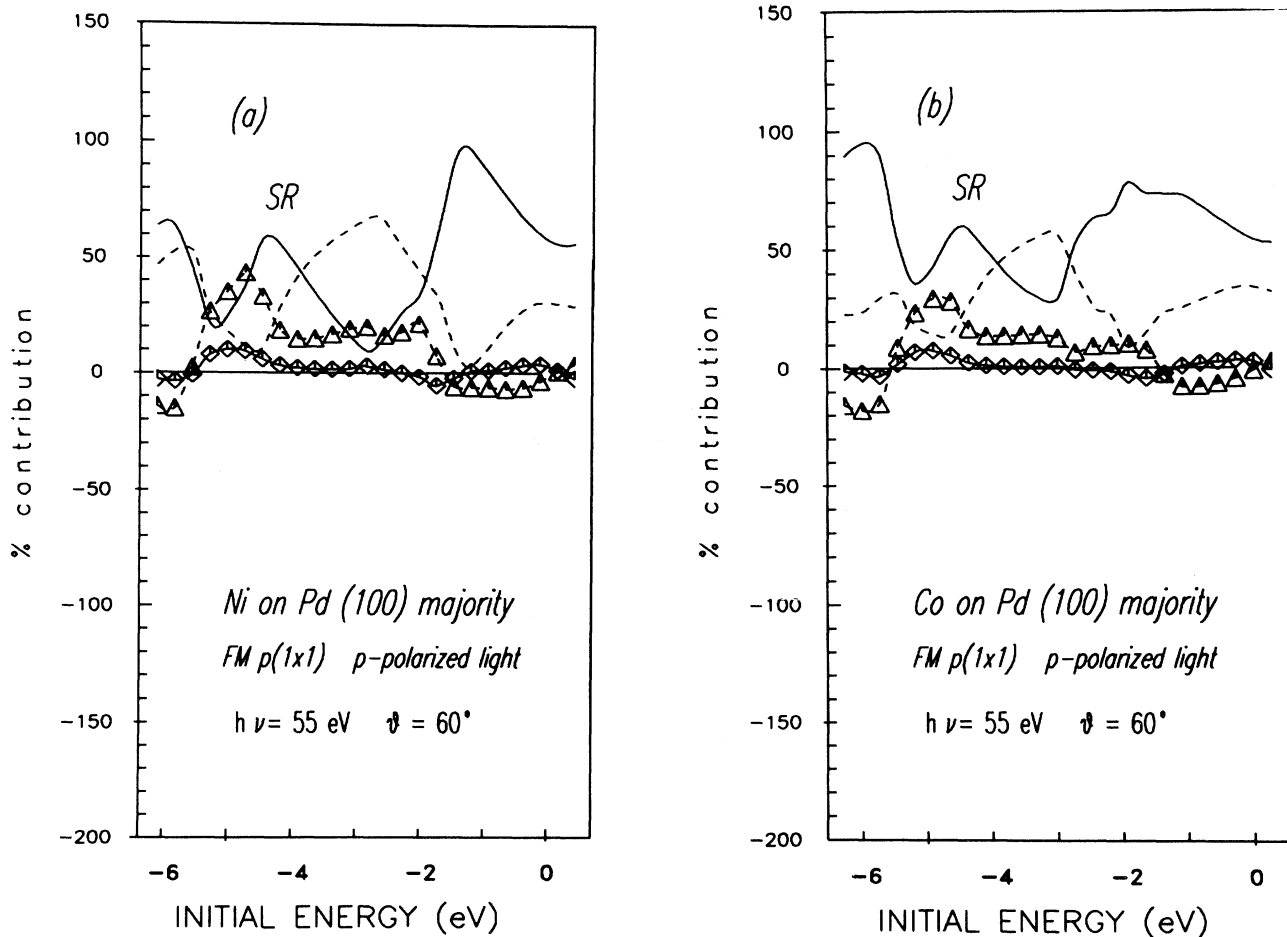


FIG. 7. Layer-by-layer distribution of the photocurrent for  $p$ -polarized light and majority spin. Solid line, layer 1 ( $3d$  metal); dashed line, layer 2 (first Pd layer); triangles, layer 3; diamonds, layer 4. (a) Ni for 55 eV, (b) Co for 55 eV, (c) Co for 65 eV.



ers. As in the case of Ni, with increasing photon energy, the influence of the first layer contribution to the Pd  $\Delta_5$  peak and the newly generated peak increases. This in turn leads to a weakening of the  $\Delta_1$  peak. In the case of Fe [Fig. 6(a)] the latter peak is almost extinguished.

For Ni [Fig. 6(c)] the differences to the spectra from the clean Pd(100) system are not very pronounced. The peaks are generally a little broader. The influence of Ni increases with increasing photon energy, leading thus to an even larger broadening. In the layer-by-layer distribution of the photocurrent [Fig. 7(a)] the same trend is seen. For low photon energies contributions from the second layer (i.e., the first Pd layer) are more dominant than contributions from the first layer. With increasing photon energy the first layer contributions gain influence. Especially for photon energies above 45 eV the first layer contribution to the surface resonance is pronounced. Correspondingly, in the spectra a shift of about 0.2 eV to higher energies is found. Just below the Fermi level an additional feature arises. The layer-by-layer distribution

reveals that for these photon energies the contribution from the two topmost layers is increasing. This feature could therefore be either an excitation from a Ni-induced surface state, or an excitation from a hybridized Ni-Pd state, or from the Pd  $\Delta_1$  band close to the Fermi level. The last possibility is most unlikely since the clean Pd spectra show no indication for such a peak.

### B. Minority-spin direction

For the minority-spin direction all three 3d metals show basically the same spectra. Only small shifts in peak positions occur.

In the case of *s*-polarized light (Fig. 8) they mainly differ from each other in the relative strength of the excitations above 40 eV photon energy, where for Ni a dominant peak just below the Fermi level is seen, whereas for Fe the second (Pd related) peak still has a remarkable intensity. The layer-by-layer distribution of the photocurrent (Fig. 9) suggests this last peak to be an overlayer-

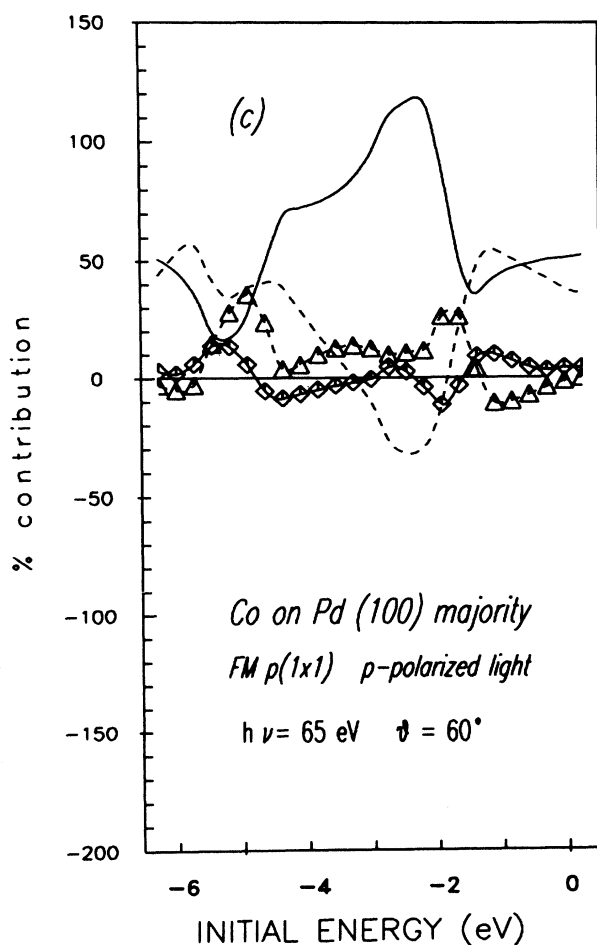


FIG. 7. (Continued).

induced surface state, since the first layer contribution (i.e., the contribution of the  $3d$  metal) is restricted to the energy range from the Fermi energy to about  $-2$  eV binding energy.

The spectra for  $p$ -polarized light are presented in Fig. 10. For Fe [Fig. 10(b)] there are only a few deviations from pure Pd(100) found for the features just below the Fermi energy. In general the Pd  $\Delta_1$ - $s$ -band peak is less affected by the overlayer than for majority-spin direction. The layer-by-layer distribution (Fig. 11) confirms again the almost pure Pd origin of this feature. The surface resonance, however, is shifted considerably by about 0.6

eV to higher energies and is much more pronounced. As in the majority case we find an enhancement of the first layer contribution to the photocurrent. The Pd  $\Delta_5$  peak is enhanced, especially in the case of Fe, but not as much as in the majority-spin spectra. The main contributions to this peak come from the topmost Pd layers. The Pd  $\Delta_1$  peak is slightly shifted by 0.2 eV to higher energies. For high photon energies this peak vanishes due to the more dominant new peaks.

At a binding energy of  $-0.7$  to  $-1.1$  eV a new peak arises. Its main contributions come from the first and second layer, indicating a mixed  $3d$ -overlayer Pd band. The second new feature emerges just below the Fermi level. This peak is mainly due to contributions from the first layer; therefore we tend to call it to a purely overlayer induced state. In the case of Fe, the Fermi energy cuts just between these two new peaks and only the hybridized state is observed. Both new peaks have  $\Delta_1$  symmetry, since they are not seen for  $s$ -polarized light.

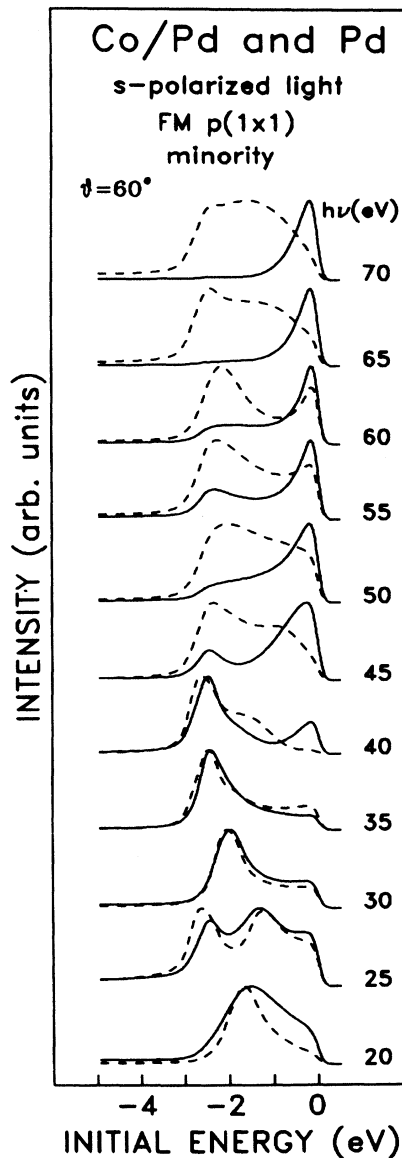


FIG. 8.  $s$ -polarized minority-spin spectra for a Co overlayer on Pd(100) (solid line) in comparison to clean Pd(100) (dashed line).

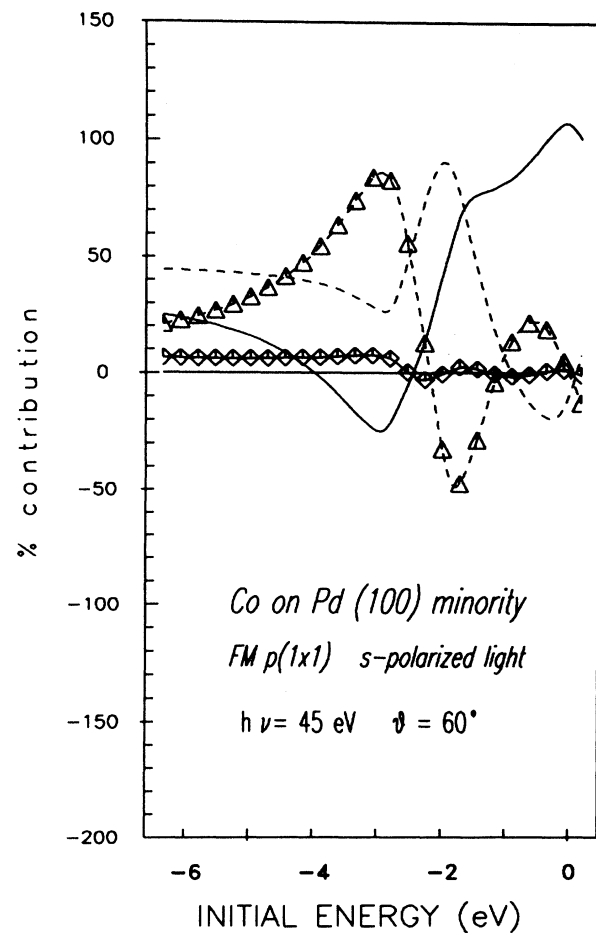


FIG. 9. Layer-by-layer distribution of the photocurrent for  $s$ -polarized light for a Co overlayer and minority spin. Solid line, layer 1 ( $3d$  metal); dashed line, layer 2 (first Pd layer); triangles, layer 3; diamonds, layer 4.

### C. Spin-integrated spectra and comparison of minority- and majority-spin direction

The spectra in Figs. 12 and 13 are spin-integrated spectra summed over both spin directions.

For the *s*-polarized majority-spin spectra the intensity of the lowest peak is decreasing from Fe to Ni, whereas the intensity of the second lowest peak is increasing. For Co both peaks are not separated. The intensity of the

highest peak is increasing too, from Fe to Ni. The lowest minority peak is too weak for high photon energies to give significant contributions.

In the case of *p*-polarized light the spin-integrated spectra of Ni differ clearly from the spectra for Co and Fe. This is mainly due to the lack of the overlayer induced states between  $-2$  and  $-3$  eV binding energy for Ni. For Co and Fe even the relative intensities of the minority- and majority-spin contributions are similar.

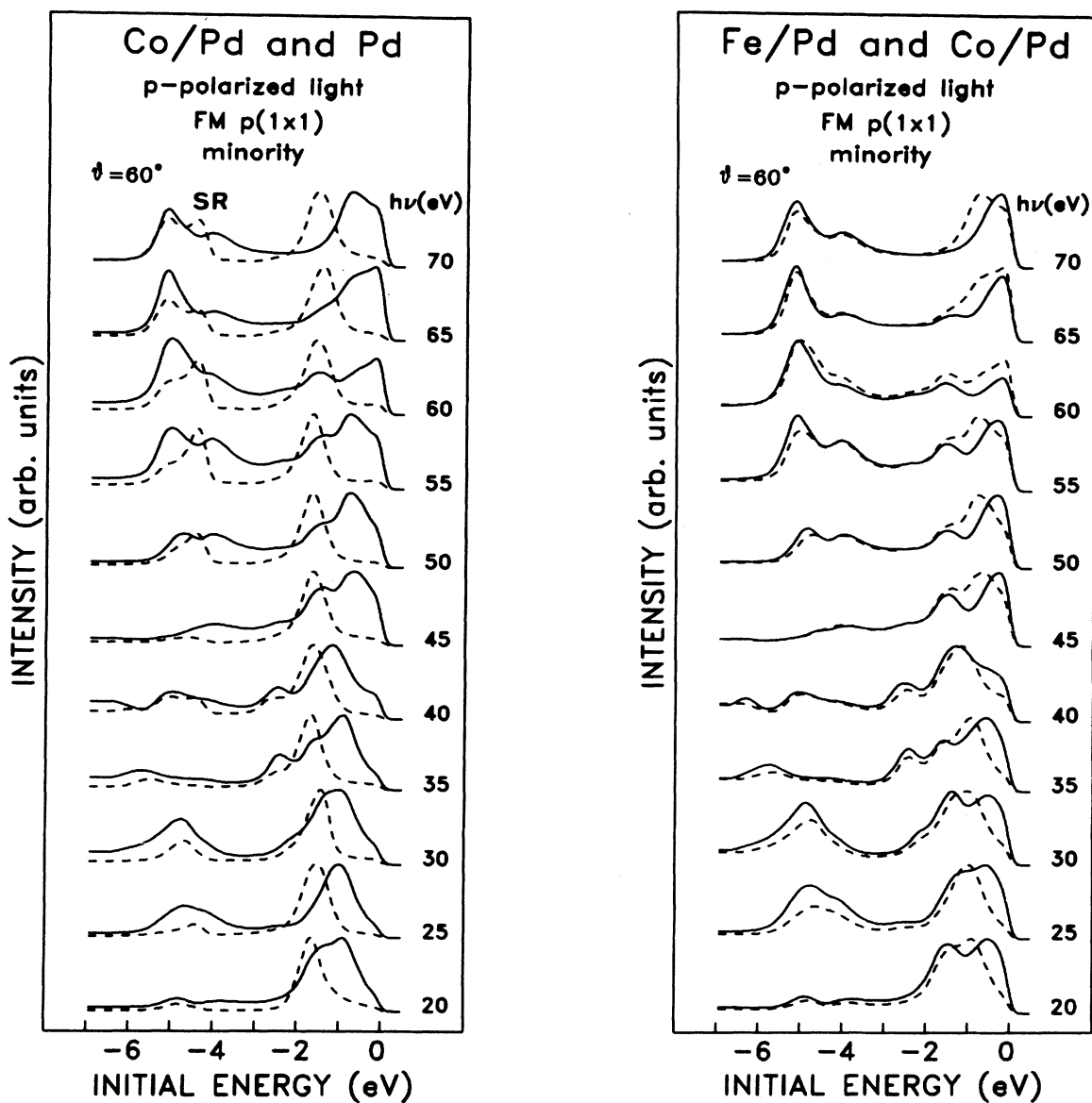


FIG. 10. *p*-polarized minority-spin spectra for (a) a Co overlayer on Pd(100) (solid line) in comparison to clean Pd(100) (dashed line), (b) comparison of an Fe overlayer (solid line) with a Co overlayer (dashed line) on Pd(100).

Since for high photon energies (about 60 eV) the escape depth is already quite small one would expect to see more of the overlayer influence, whereas for low photon energies the surface near regions and hence the Pd influence is larger. This assumption is confirmed by the layer-by-layer distribution of the photocurrent. In the following we will therefore try to discuss the meaning of the term "exchange splitting" within the framework of photoemission.

From the LDOS calculations of Blügel<sup>1</sup> follow that the Stoner model is only approximately valid and the shift of minority and majority bands is not rigid. In order to extract the "exchange splitting" in photoemission there is the problem of an unambiguously defined origin of the minority- and majority-spin peaks. The value of the "exchange splitting" not only changes from the bulk to the

surface but also with respect to different regimes of  $k_{\parallel}$ . For example, from the spectra at 70 eV and  $s$ -polarized light information specific for the  $3d$  overlayer at minimized Pd influence can be extracted. We can assume that both the minority and the majority peak are due to the  $\Delta_5$ -band excitation near  $\Gamma$ . In this particular case we find an exchange splitting, between corresponding peaks of about 2 eV for Fe, 1.8 eV for Co, and about 1.2 eV for Ni. In the case of  $p$ -polarized light the same values can be extracted. However, even in this particular setup no unique exchange splitting can be extracted, since the shifts between minority and majority peaks are not completely rigid. Therefore extreme caution should be exercised in extracting the "true exchange splitting" from photoemission spectra. The general trend shows a decreasing exchange splitting going from Fe to Ni. This finding is in qualitative agreement with the prediction of Blügel.<sup>1</sup> They find that the magnetic moment decreases in steps of  $1\mu_B$  from Mn to Ni because charge neutrality is achieved by adjusting the population of the minority band.

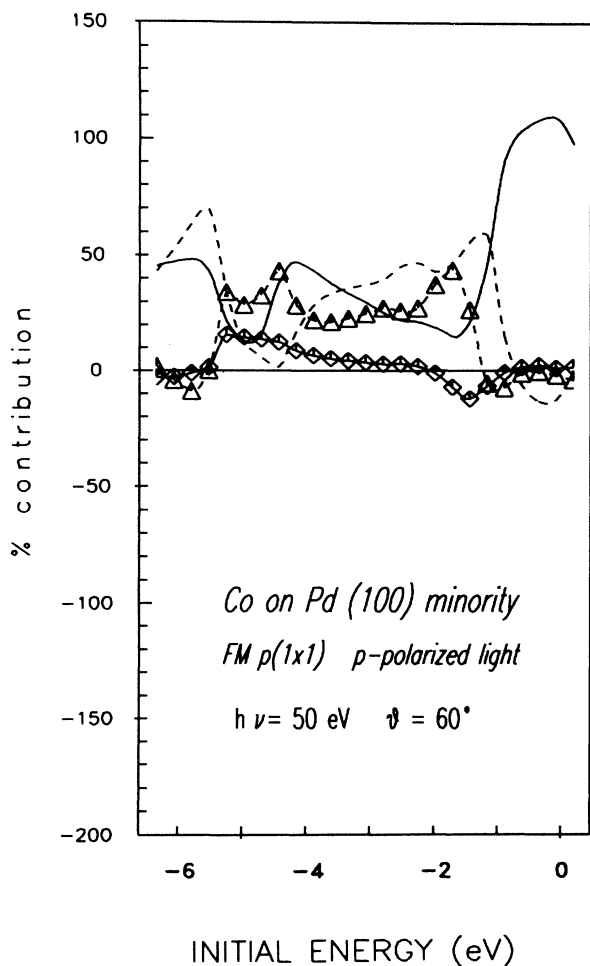


FIG. 11. Layer-by-layer distribution of the photocurrent for  $p$ -polarized light for a Co overlayer and minority spin. Solid line, layer 1 ( $3d$  metal); dashed line, layer 2 (first Pd layer); triangles, layer 3; diamonds, layer 4.

## VII. SUMMARY

In the case of the majority-spin direction Co and Fe overlayers behave very similarly, whereas the Ni overlayer yields a completely different spectrum. For  $s$ -polarized light the new  $\Delta_5$  state in the Co- and Fe-overlayer systems has a binding energy of  $-2.5$  eV, which is about the same as the  $\Delta_5$  peak in pure Pd. For Ni the new  $\Delta_5$  peak is found at about  $-1.5$  eV. In the case of  $p$ -polarized light there is no new feature in the Ni spectra. The Ni-overlayer  $\Delta_5$  peak and the Pd  $\Delta_1$  peak have the same binding energy. For Co and Fe a peak with  $\Delta_1$  symmetry is found dispersing between  $-2.0$  and  $-2.4$  eV. From the layer-by-layer distribution of the photocurrent it is evident that this peak is strongly influenced by the overlayer.

In the case of the minority-spin direction the spectra for Fe, Co, and Ni overlayers show the same features. For  $s$ -polarized light a peak with  $\Delta_5$  symmetry arises just below the Fermi energy and in the case of  $p$ -polarized light there are two new peaks, both with  $\Delta_1$  symmetry. The lower one, at a binding energy of about  $-0.8$  to  $-1.0$  eV exhibits more influence from the Pd substrate than the second one at about  $-0.2$  eV.

In accordance with the predictions of Blügel<sup>1</sup> the influence on the majority spectra is stronger than for the minority-spin direction. This in fact was to be expected also from the different nature of hybridization for the two spin directions. Some indications about the hybridization might have even been drawn from the bulk band structure of bcc Fe, fcc Co, and fcc Ni in comparison to Pd. The exchange splitting in the bulk band structure reflects the occupation of the bands. For the majority-spin direction in all three metals there are only very small differences in the  $\Gamma_{12}$  and  $\Gamma_{25}$  energy levels and a little larger differences for  $X_2$  and  $X_5$ . For Ni the same is valid

also for the minority-spin direction especially for  $X_2$  and  $X_5$  where the smallest deviations are found. In contrast to Ni in Fe and Co the minority bands are shifted appreciably higher in energy which makes hybridization more unlikely. This might explain the observed difference between the minority spectra of Ni to those of Fe and Co. This hybridization effect seems to be even strong enough to make up for the differences between bcc Fe and fcc Co.

Since the minority bands are shifted to a large extent above the Fermi level, from photoemission no conclusion can be drawn about the importance of hybridization. For Fe and Co a minority LDOS peak has its center of gravity just above the Fermi energy. In the spectra (Fig. 10) the onset of a corresponding peak is found. It is hardly visible in the case of Fe but already quite distinct in the case of Co.

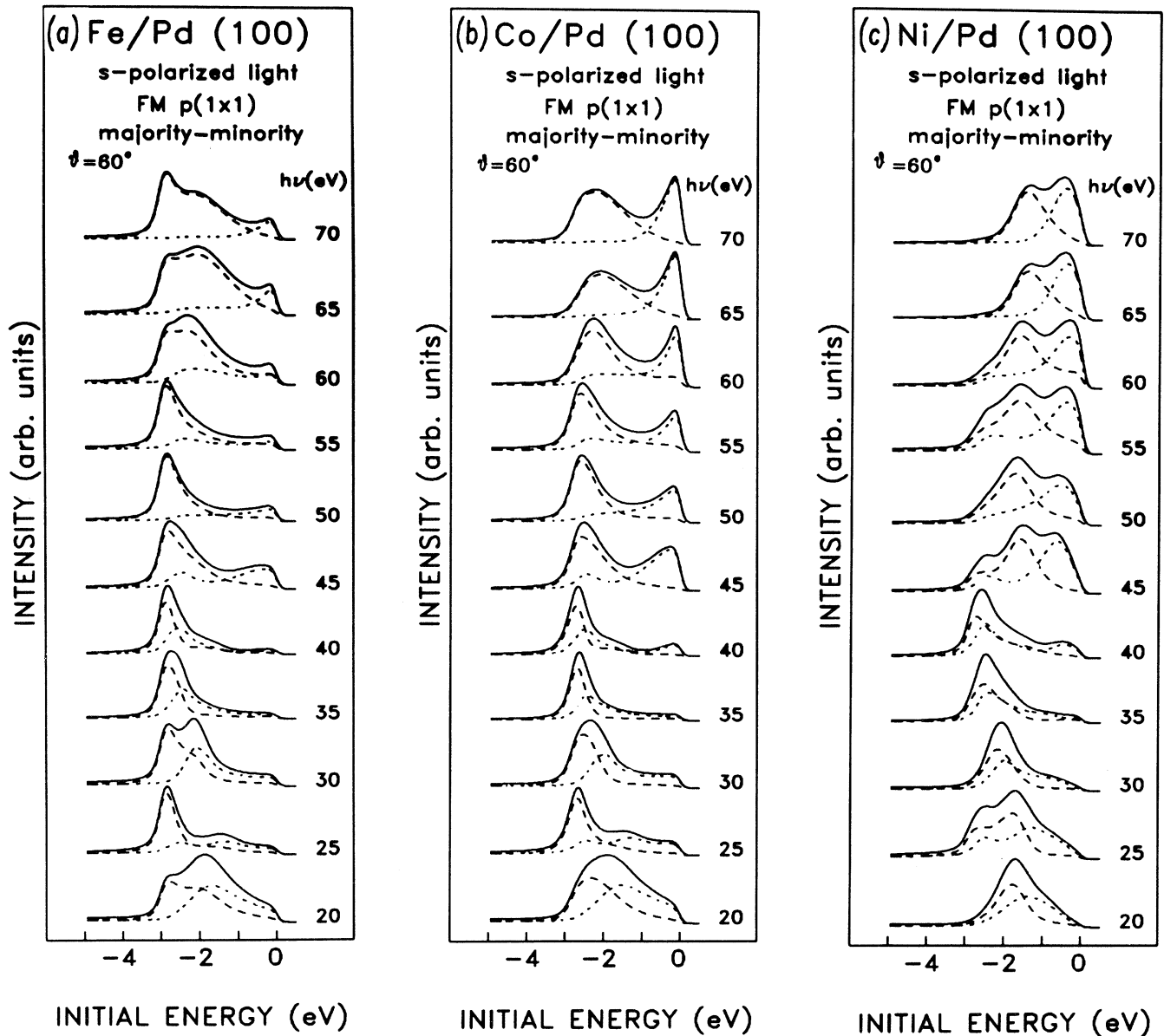


FIG. 12. Spin-integrated spectra (solid lines) together with the minority- (dotted lines) and majority- (dashed lines) spin contributions for s-polarized light for (a) an Fe overlayer, (b) a Co overlayer, and (c) a Ni overlayer on Pd(100).

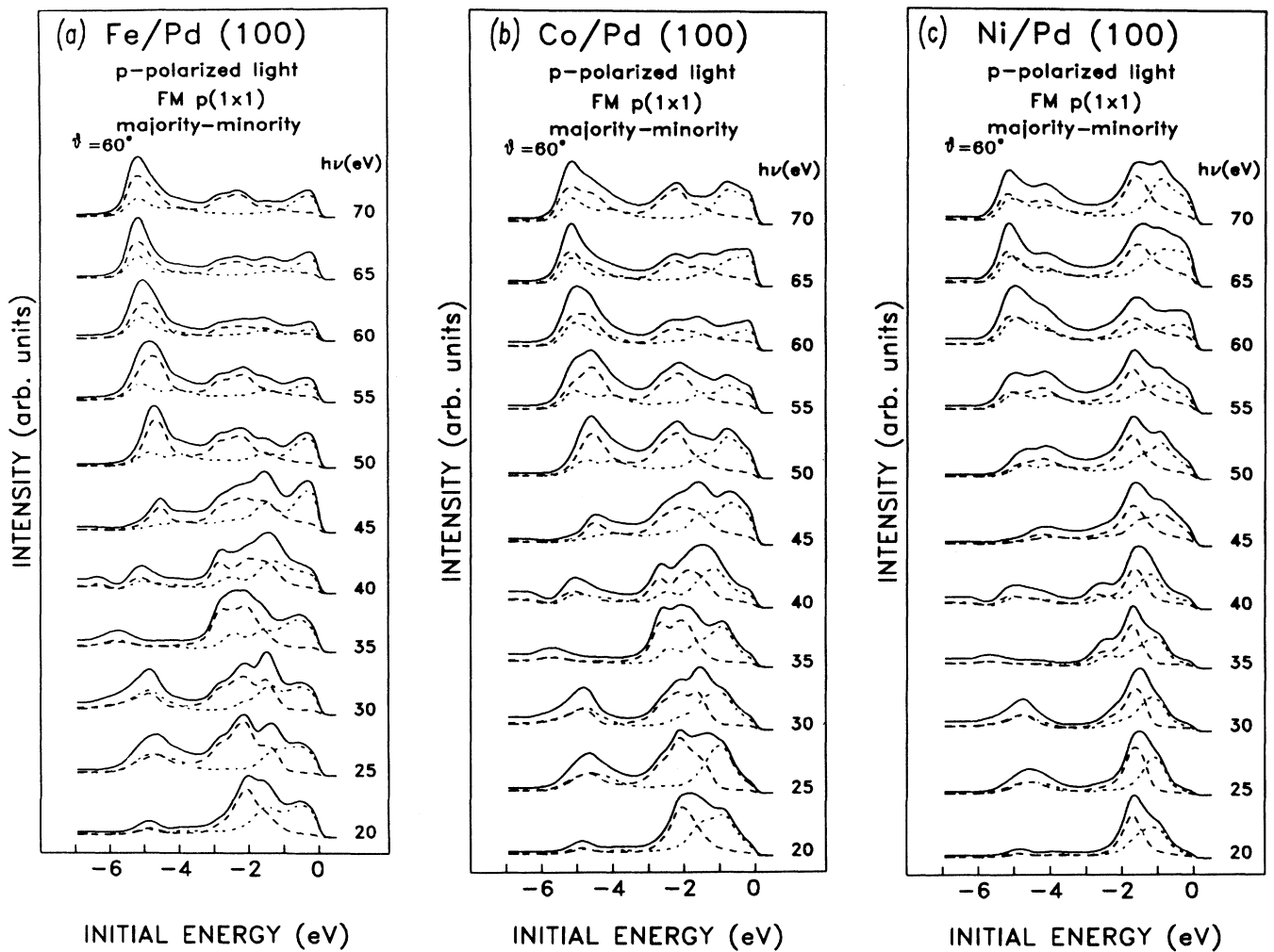


FIG. 13. Spin-integrated spectra (solid lines) together with the minority- (dotted lines) and majority- (dashed lines) spin contributions for  $p$ -polarized light for (a) an Fe overlayer, (b) a Co overlayer, and (c) a Ni overlayer on Pd(100).

The exchange splitting is decreasing from Fe to Ni by about 0.8 eV. Blügel<sup>1</sup> found values of about  $1\mu_B$  for Ni to  $4\mu_B$  for Mn and correspondingly much larger splittings for the local DOS.

We hope that the present calculation will encourage new photoemission experiments on these interesting monolayer systems.

#### ACKNOWLEDGMENTS

The authors are very grateful to Professor P. H. Dederichs for his interest in this project. This paper was partially supported by the Austrian Ministry of Science (Zl. 49.554/1-27a/88) and by the Jubiläumsfonds der Stadt Wien.

<sup>1</sup>S. Blügel, *Europhys. Lett.* **7**, 743 (1988).

<sup>2</sup>S. Blügel and P. H. Dederichs, *Europhys. Lett.* **9**, 597 (1989).

<sup>3</sup>S. Blügel, D. Pescia, and P. H. Dederichs, *Phys. Rev. B* **39**, 1392 (1988).

<sup>4</sup>S. Blügel, M. Weinert, and P. H. Dederichs, *Phys. Rev. Lett.*

**60**, 1077 (1988).

<sup>5</sup>S. Blügel, M. Weinert, and P. H. Dederichs, *Phys. Scr. T* **25**, 301 (1989).

<sup>6</sup>S. Blügel, B. Drittler, R. Zeller, and P. H. Dederichs, *Appl. Phys. A* **49**, 547 (1989).

- <sup>7</sup>G. Bergmann, *Phys. Rev. B* **23**, 3805 (1981).
- <sup>8</sup>J. F. L. Hopkinson, J. B. Pendry, and D. J. Titterton, *Comput. Phys. Commun.* **19**, 69 (1980).
- <sup>9</sup>J. B. Pendry, *Surf. Sci.* **57**, 679 (1976).
- <sup>10</sup>J. B. Pendry, in *Low Energy Electron Diffraction*, edited by G. K. T. Conn (Academic, London, 1974).
- <sup>11</sup>U. König, P. Weinberger, J. Redinger, H. Erschbaumer, and A. J. Freeman, *Phys. Rev. B* **39**, 7492 (1989).
- <sup>12</sup>R. Hora and M. Scheffler, *Phys. Rev. B* **29**, 692 (1984).
- <sup>13</sup>N. V. Smith, *Phys. Rev. B* **9**, 1365 (1974).
- <sup>14</sup>N. E. Christensen, *Phys. Rev. B* **14**, 3446 (1976).
- <sup>15</sup>F. M. Müller, A. J. Freeman, J. O. Dimmock, and A. M. Furdyna, *Phys. Rev. B* **1**, 4617 (1970).
- <sup>16</sup>G. C. Smith, C. Norris, C. Binns, and H. A. Padmore, *J. Phys. C* **15**, 6481 (1982).
- <sup>17</sup>M. Pessa and M. Vulli, *J. Phys. C* **16**, L629 (1983).
- <sup>18</sup>D. G. O'Neill and J. J. Joyce, *J. Vac. Sci. Technol. A* **3**(3), 1639 (1985).
- <sup>19</sup>R. H. Stulen, T. E. Felter, R. A. Rosenberg, M. L. Knotek, G. Loubriel, and C. C. Parks, *Phys. Rev. B* **25**, 6530 (1982).
- <sup>20</sup>D. R. Lloyd, C. M. Quinn, and N. V. Richardson, *Surf. Sci.* **63**, 174 (1977).